Effect of matrix damage on compressive strength in the fiber direction for laminated composites

G. Eyer[a], O. Montagnier[a,b,*], C. Hochard[a], J-P. Charles[a]

[a]Aix Marseille Univ, CNRS, Centrale Marseille, LMA, Marseille, France
[b]Centre de Recherche de l'Armée de l'Air, Ecole de l'air, B.A. 701, 13661 Salon-Air, France

Abstract

An original experimental method is proposed to characterize the influence of matrix damage on the compressive strength of laminated composites in the fiber direction using tubes. These composite tubes have a dumbbell-shaped geometry so that rupture occurs in the specimen center without stress concentration. They can be constituted of unidirectional or woven plies aligned with the axial direction. First, a torsional cyclic load is applied in order to damage the matrix. This damage is measured at the tube scale via the reduction in shear modulus. Second, a compressive load is applied up to failure for various damage levels.

The method is applied to a woven carbon/epoxy material. Results show that the matrix damage affects significantly the compressive strength in the fiber direction. It is yet observed that longitudinal stiffness is not modified by damage. Finally, a simple model is proposed to describe this decrease of strength vs. matrix damage.

Keywords: A. Polymer-matrix composites (PMCs), B. Strength, C. Damage mechanics, D. Mechanical testing

1. Introduction

One of the main issues in engineering design of composites is the prediction of failure. In the case of composites, the mechanisms of collapse are manifold [1]. For many years, the introduction of damage mechanics has made it possible to successfully describe the progressive failure of the matrix especially observed in the case of fatigue loads [2–4]. Matrix damage is associated with the growth of micro-cracks in the resin and the development of fibre/matrix debonds and transverse cracks. This leads to the decrease in the stiffness in transverse and shear directions at the ply scale. A matrix damage variable d is generally introduced to quantify this stiffness reduction. Most of the time, these cracks do not lead to the global failure of the laminates. Contrarily, the failure of fibers generates a sudden and catastrophic collapse of the laminates.

Even if the growth of damage does not directly cause the failure of the laminate, it can significantly affect the strength of the ply in the fiber direction. Indeed, in a previous work it was experimentally measured that matrix damage causes a drop in the tensile strength [4, 5]. This work was performed on tubes made of Glass/Epoxy unbalanced woven plies. First, a torsion cyclic loading was applied to generate matrix damage. Then, tensile tests were performed to measure the tensile strength. These tests show that the final strength can be equal to the third of the initial strength when damage is high [4, 5]. The model proposed by Hochard *et al.* [4] is that the strength evolves sharply between two values according to a damage threshold value ($d \gtrsim 0.8$).

In a similar way, the aim of this paper is to study the effect of matrix damage on compressive strength in the fiber direction for laminated composites. Interesting work by Gibson *et al.* [6] shows that the progressive increase in temperature of a glass/polypropylene composite leads to the progressive reduction in compressive strength in the fiber direction. This behavior is directly linked to the drop in matrix modulus. Since matrix damage increase has a similar effect on this modulus, we can imagine that this increase will also lead to the decrease in compressive strength in the fiber direction. These authors also observed that when the matrix is completely burned, the failure in compression of the composite in the fiber direction is obtained for an extremely low stress.

Micro-models give interesting pieces of information about the effect of damage on compressive strength. Rosen [7] has postulated that elastic micro-buckling of the fibers was responsible for the collapse of the ply. This model gives an analytic solution for the compressive strength (see the list of nomenclatures for the symbol definitions):

$$\sigma_c = \frac{G_m}{1 - \nu_f} \approx G_{12} \tag{1}$$

This equation shows that the most significant parameter in compressive failure is not linked to the fibers but is linked to the stiffness of the matrix. On the other hand, it is well known in damage mechanics [1] that the actual modulus is proportional to the matrix damage, which means that:

$$G_{12}(d) = G_{12}^0 (1 - d) \tag{2}$$

By coupling the equations above, it is shown analytically that the compressive strength is proportionally affected by the matrix damage as follows:

$$\sigma_c(d) = G_{12}^0 (1 - d) \tag{3}$$

---

*Corresponding author

Email address: `olivier.montagnier@defense.gouv.fr` (O. Montagnier)

Rosen's model gives an interesting result but the predicted value is not in good agreement with experiments. Many other models have then been developed to improve this prediction by considering the failure as a plastic instability generating a kink-band [8–11]. These models are able to take into account an increasing number of physical phenomena and geometrical defects, e.g., plasticity, matrix damage, fiber misalignment, etc. In particular, Kulkarni et al. [12] and Steif [13] have investigate the influence of the lack of perfect bond between fibre and matrix. Kulkarni et al. show theoretically the large degrading influence of the interface condition on the compressive strength. On the other hand, the experimental validation of these models remains complex because of the difference in scale between the micro models and the experiments (generally at the meso scale). In any case, literature on micro models shows that the state of the matrix is essential in the prediction of the compressive strength.

In this paper, experimental research is proposed in order to quantify the effect of matrix damage on compressive strength for carbon fiber reinforced plastics (CFRP) in the fiber direction. First, the choice of the proposed experimental method will be explained. This method must be able to impose a certain level of damage and to apply compression in the fiber direction up to failure. Then, the experimental setup will be described. Experimental results on undamaged and damaged specimens will be presented and analyzed. Finally, a simple model adapted to an engineer approach is proposed. This model linked the compressive strength to the matrix damage state at the meso scale.

2. Experimental method

2.1. Choice of the experimental method

The aim of this work is to study the influence of transverse damage on the compressive behavior in the fiber direction for laminate composites. To address this problem, it is necessary to propose an experimental method that would make it possible to damage the matrix as well as achieve compression in the fiber direction. Two approaches are possible: one consisting in providing one single experimental setup for both steps and the other consisting in providing one experimental setup for each step.

The compression tests are particularly complex to perform in comparison with tensile tests because of the risk of specimen buckling. The classical compression test, also called Celanese test, is also known for its defects. The results generally highlight low ultimate compressive strain and exhibit high variability mainly because of specimen buckling and large stress concentration at the tabs [14, 15]. Many modified compression tests have been proposed to overcome these defects [6, 16–18]. Despite these improvements, these tests seemed unfavorable for a detailed study of the influence of damage on the ultimate compressive strain.

The other experimental method to study the behavior in compression of laminate composites is the bending test. There are many types of bending tests: classical bending tests with three points [11] or four points [19–21], or more exotic tests like pure bending tests [15, 22] and constrained buckling tests [23]. Conventional bending tests generally give higher ultimate compressive strain values. However they show two difficulties: the computation of the stress field requires a complex inverse problem due to the large displacements and the stress concentrations introduced at the support points can lead to premature failure of the specimen. Montagnier et al. [15] and then Bois et al. [22] proposed a pure bending test with a dumbbell-shaped specimen in order to circumvent these difficulties. In this case, the bending moment value is perfectly known without assumption, which simplifies the computation of the stress field. In addition, the dumbbell-shaped geometry allows the rupture to be located in the center of the specimen without stress concentration. Finally, Wisnom et al. [23] proposed a constrained buckling test that also achieves very high ultimate compressive strain. Note further that bending tests involve a strain gradient effect in the thickness of the specimen, widely described in the literature [11, 23, 24]. The stability and precision obtained with bending tests seem to be suitable for the proposed study. However, bending specimens must be especially long and damaging this kind of specimen, with shear for example, seems to be complex to carry out.

Previous tests do not seem satisfactory to our study, we propose then a test on dumbbell-shaped composite tubes constituted of plies positioned at 0 ° relative to the tube axis. The method is applied here to balanced woven plies. The tubular shape makes it possible to both damage the matrix in shear with a torsion test and then perform a pure compressive test in the fiber direction. This test allows a homogeneous field and therefore a simple calculation for the stress. Specimens of similar form had already been used by Hochard et al. [4] to achieve shear/tension tests. Nevertheless the compression test is problematic for the aforementioned reasons (buckling and stress concentration), a careful development of this test in the case without damage is proposed in [25–27].

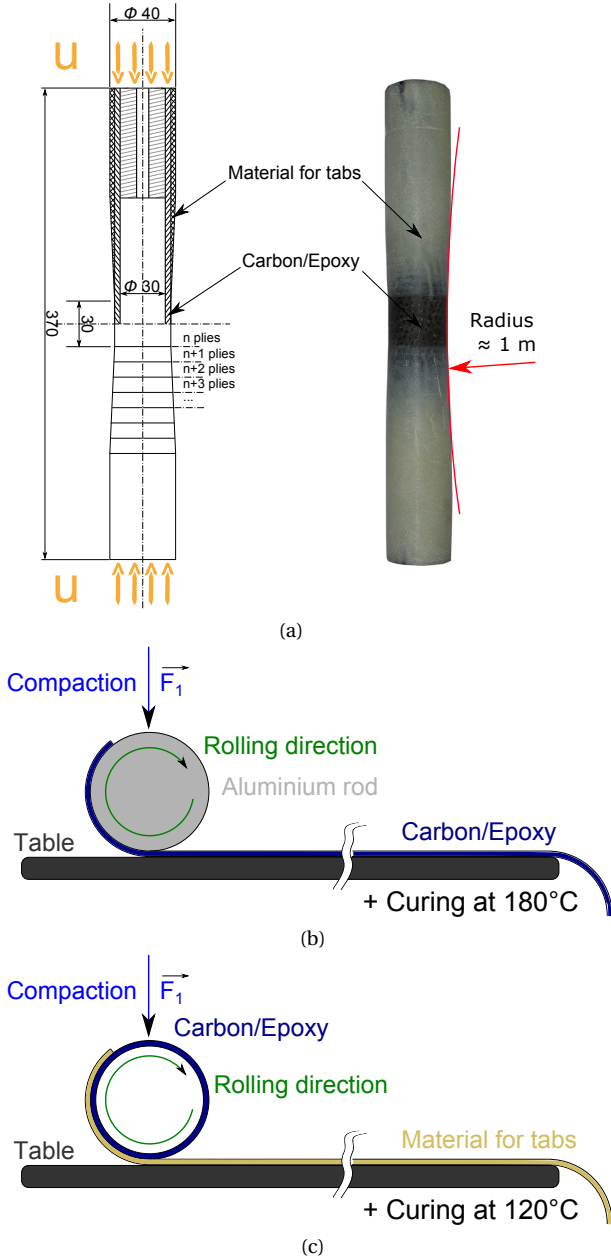## 2.2. Specimen preparation

Figure 1: Manufacturing and geometry of the samples: (a) geometry of the sample (b) step 1 – rolling carbon tube (c) step 2 – rolling tabs

As it is mentioned above, the specimens used in this study are dumbbell-shaped composite tubes (Fig. 1a). Their external diameter is set to 40 mm by the testing machine. In order to generate a large radius (approximately equal to 1 m, see Fig. 1a), the length of the specimen must be large enough and set to a value of 370 mm.

Tubes are manufactured in two steps. First, a tube made of balanced woven carbon/epoxy (G939/M18 (Table 1)) is manufactured using a wrap rolling process [28]. The weave is a 4-Harness Satin. The standard designation is HTA for the fibers and M18 for the resin. The method consists in rolling prepreg plies around an aluminum rod, as presented in Fig. 1b. This aluminum rod is the internal mold. During rolling, a force is applied in order to compact the plies. Finally, the external ply is a heat-shrinkable tape, whose shrinking during curing ensures compaction.
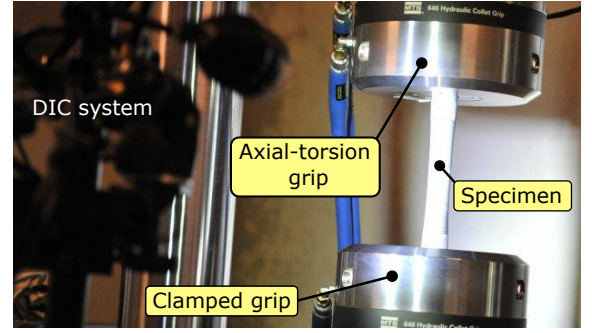

Figure 2: Specimen installed in the axial-torsion universal testing machine (MTS 322)

For this type of resin, a curing cycle at 180°C is imposed. This method is only possible when the thermal coefficient of aluminum is greater than that of the composite. This allows the aluminum rod to be removed after the curing cycle. The internal diameter of the tube is set at 30 mm, based on the diameter of the rod. The quasi-perfect cylindricity of the rod makes it possible to consider the cylindricity defect of the tube as negligible. The stacking sequence of the tube is $[0°]_{11}$ in order to avoid buckling and the thickness is equal to 2.75 mm [27].

Next, the carbon tube is reinforced with tabs at both ends so that the crack occurs in the gauge area, which is the zone where the tube is not reinforced (Fig. 1c). The shape of the tube is then turned into that of a dumbbell. To obtain this shape, the number of plies is progressively increased to match the dimensions of the clamp (Fig. 1a). Tabs are made with $[90°]$ plies of unbalanced woven glass/epoxy. The design of the tabs of the specimens is detailed more precisely in [27].

The external coaxiality of the clamped end cannot be controlled during the curing process because the proposed method does not use an external mold. Yet if this coaxiality is too low then bending can appear during the compressive test, which will dramatically affect the results. For this reason, the external face of the tube tabs is machined on a lathe. To avoid local damage, the dumbbell-shaped section and the gauge section of the tube are not machined. In order to keep the coaxiality, the specimen is guided internally.

Finally the clamped ends of the specimen are filled with an aluminum rod to avoid the failure caused by the tightening of the machine.

2.3. Experimental set up and methods

The experimental setup is based on a axial-torsion universal testing machine (Fig. 2). In order to check the homogeneity of the strain field in the sample, the test is followed by 3D Digital Image Correlation (DIC) [29]. Two cameras are needed in order to take into account the non flatness of the sample. The image speed is 2 images per second. This number of images per second is adapted to follow the behavior of the material during the test but it is not enough to access the mechanisms of failure. Figure 3 gives a description of the 3-step protocol.

In the first step, torsion is applied to the tube specimen in order to shear the matrix and thus, to create diffuse damage. In the case of carbon/epoxy woven plies it is not possible to
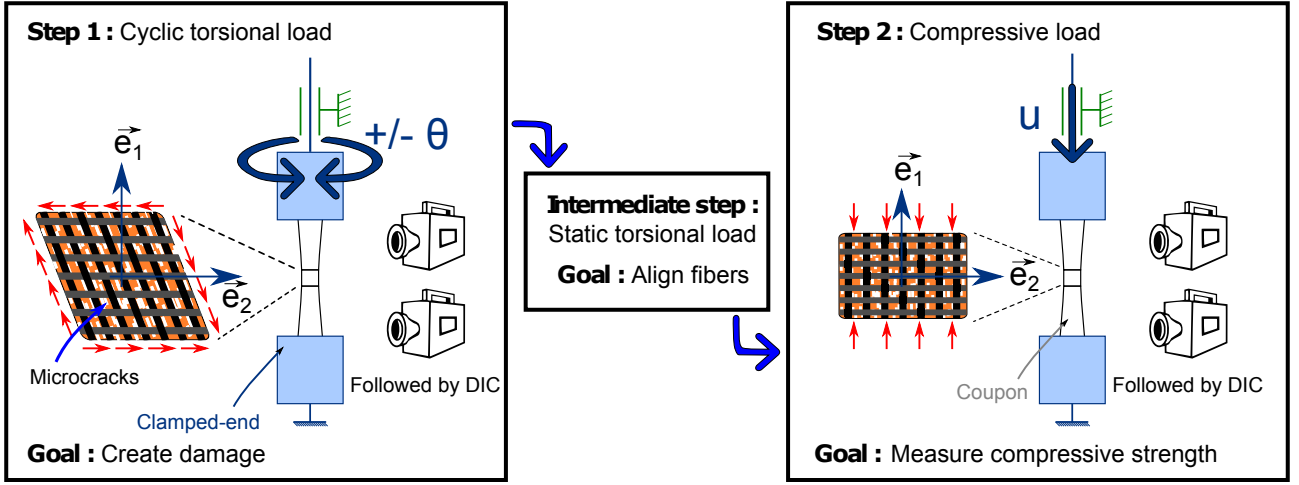
Figure 3: Illustration of the different steps of the experiment

create damage of more than 0.5 with a static load because the stiffness reduction leads to material instability [1]. That is why it is necessary to use a cyclic load. This step is then performed at a cyclic rotation of 1 °/sec with various amplitude angles from −5° to +5°. The common number of cycles is 500. The damage is measured after each step of 500 cycles. The method to measure the damage is based on the measure of the stiffness reduction and will be detailed in the next section. This procedure is repeated while the value of damage is not targeted.

When the value of damage is considered to be enough, the torsion cycles are stopped and an intermediate step is started. The goal is here to realign the fibers in the gauge area along the compression load direction by using DIC. The value of the residual shear strain is measured in the sample by calculating the shear strain between the first image of step 1 and the last image of the torsion cycles. When the shear strain is too high, a static rotation is performed in order to decrease the value of the shear strain. A value of less than 0.0005 for the residual shear strain is considered as acceptable. In this case fiber misalignment is assumed negligible by comparison with the natural fiber misalignment due to the weaving architecture.

During step 2, the compressive test is performed in order to identify the behavior of the damaged material in compression and to measure the ultimate compressive strength. This step is performed at a uniform cross head displacement of 1 mm/min. The strain field in the specimen is monitored by DIC.

3. Results, modeling and discussion

3.1. Test on undamaged specimens: identification of the behavior

First, the behavior of the undamaged material is investigated up to failure. In this case, step 2 is directly applied to the tube sample.

Fig. 4 shows the longitudinal strain field of an undamaged tube just before failure. The strain is not perfectly uniform in the gauge area for three reasons: the material is not locally homogeneous due to the weaving architecture, tab reinforcements affect the strain field, and there may be mea-
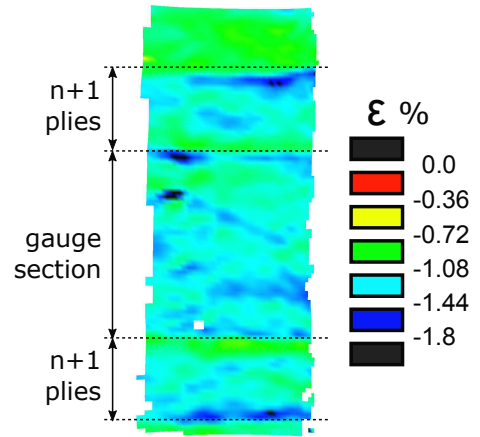

Figure 4: Compression of an undamaged tube: strain field in tube direction just before collapse
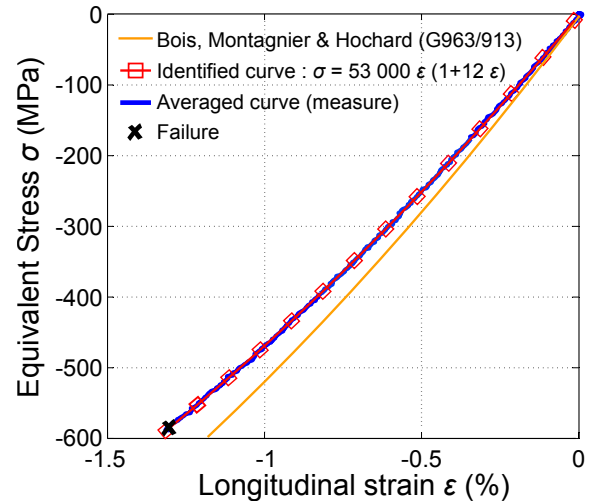

Figure 5: Non linear behavior in compression up to failure (woven carbon/epoxy material G939/M18)

surement errors in the DIC system and the speckle pattern. That is why an average strain is calculated in order to characterize the material behavior. This average is calculated at every step using MATLAB [30] after the test.
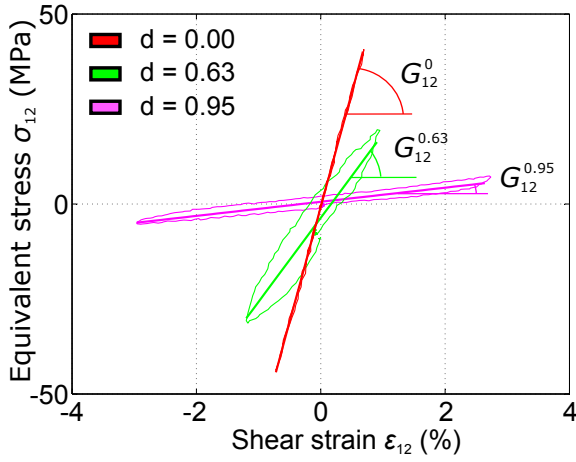
4

Figure 6: Loss of rigidity in shear direction for three different specimens after torsional fatigue cycles
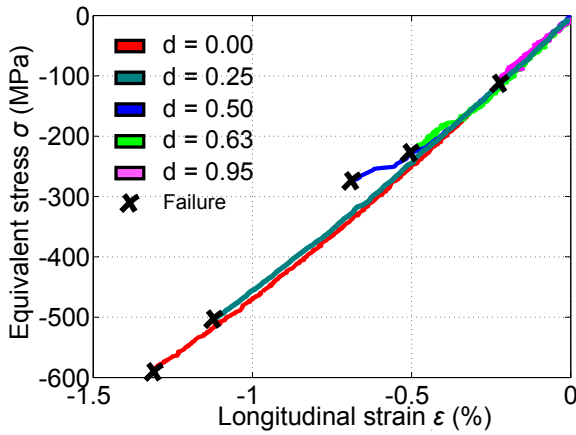

Figure 7: Behavior in compression for different damage states (woven carbon/epoxy material G939/M18)

Fig. 5 shows the plot of the experimental σ-ε curve where the equivalent stress σ corresponds to the compressive load divided by the surface of the tube cross-section. The average strain in the direction of the tube just before collapse is $\varepsilon_c^{d=0} = 1.35$ %. This value is close to the ultimate tensile strain ($\varepsilon_t^{d=0} = 1.5$ % [22]), but the ultimate stress is different in traction ($\sigma_t^{d=0} = 820$ MPa [22]) and in compression ($\sigma_c^{d=0} = 590$ MPa) because the behavior is significantly non linear in compression.

The model proposed by Allix *et al.* in [19] and identified in [15, 22, 31] is used here in order to model this non linear behavior:

$$\sigma = E_{11}^0(1 + \alpha\varepsilon)\varepsilon \qquad (4)$$

The identified values for the Young modulus E_{11}^0 and the non linear parameter α are 53000 MPa and 12, respectively. The identified curve is plotted in Fig. 5. It appears that the stiffness reduction model used here is in good agreement with the experimental data. Moreover, the values of the co-efficients identified with this experiment are close to those identified with a pure bending test in [22] on a similar carbon balanced woven ply (G963/913).

3.2. Test on damaged specimens: effect of damage on ultimate compressive strain

The effect of matrix damage on the compressive strength is now studied. Composite tubes are damaged with cyclic torsional load, as is explained in 2.3. At the end, a full torsion cycle at low speed is used to measure the loss of shear stiffness. The equivalent shear stress (torque divided by the surface of the tube cross-section and the mean tube radius) is plotted in Fig. 6 according to the shear strain. This shear strain in the gauge area is measured by using DIC. Curves are interpolated by a simple linear regression which exhibits a large decrease of stiffness versus the damage. It can be remark that cycle curves exhibit also a hysteresis. This effect is probably related to the viscosity and the friction in cracks and debonds, but these ones are not associated with a global stiffness reduction. As part of our simplified experimental approach, only the global change in slope is taken into account. Damage is finally calculated as follows:

$$d = 1 - \frac{G_{12}^d}{G_{12}^0} \qquad (5)$$

where G_{12}^d and G_{12}^0 are the initial and the actual in-plane shear modulus, respectively. The damage values obtained are 0.25, 0.5, 0.63 and 0.95. For visibility, only three shear curves are plotted in Fig. 6. It can be remarked that there is a shear stress gradient in the tube thickness. With a linear assumption, the difference between the stresses inside and outside the tube with respect to the middle radius is about 7%. The softening behavior of the material further reduces this difference. As part of the simplified engineering approach proposed, this measurement error is neglected.

Damaged tubes are thus ready to be tested in pure compression up to failure. This study remains essentially qualitative because composite tube manufacturing and experiments are very time-consuming. That is why it was decided to use only one tube per level of damage. In another part of our work, not described in the present paper, we developed a testing method with flat specimens [25, 32].

Fig. 7 represents the compressive behavior in fiber direction for different damaged specimens. The non linear behavior identified previously on an undamaged specimen is not modified when damage increases. Yet the compressive strength has significantly and progressively decreased. This observation confirms that failure of composites in compression is essentially due to the state of the matrix. Contrarily, the stiffness in fiber direction is not affected by increasing the value of the damage. The fact that rigidity in compression is not modified means that fibers are not broken during the torsional cycles and the compression load path.

Figs. 8 and 9 show pictures of fracture surfaces just after failure for two damage states. The observation is only based on a *post-mortem* observation. The crack is always localized along the whole circumference of the cylinder. The fracture surfaces for the two cases are different. However, it is still complex to identify the origin of the collapse because the failure is sudden and catastrophic, and the fracture surface is crushed.

In Fig. 10, the strain leading to failure is plotted according to the damage. A linear decrease in the ultimate compressive strain is observed when the value of damage increases. To
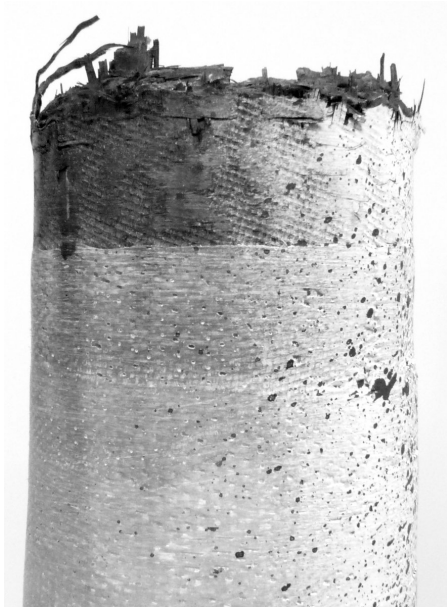
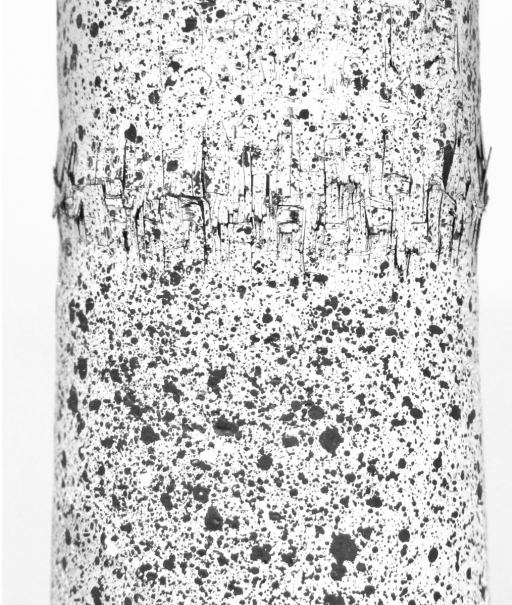Figure 8: Typical failure in compression in the middle of the gauge area for large damage specimen ($d = 0.63$)

Figure 9: Typical failure in compression in the middle of the gauge area for high damage specimen ($d = 0.95$)

take this strength reduction in future calculations, a simple linear model is proposed as follows:

$$\varepsilon_c(d) = \varepsilon_c^{d=0}(1 - d) \tag{6}$$

The extreme case d equal to 1 is complex to obtain experimentally. For this case, we assumed that the material is close to the woven dry. As a result, the compressive stiffness tends to zero, as it was observed by Gibson *et al.* in [6] for a completely burned matrix. The proposed model is very simple, adapted to an engineering approach, it is then reasonable to assume the ultimate compressive strain is null in this case. Moreover, this model is in good agreement with the expected trend by micro-models (in section 1 and [7]). An advantage of this modeling is that the identification remains really easy because it introduces just one parameter
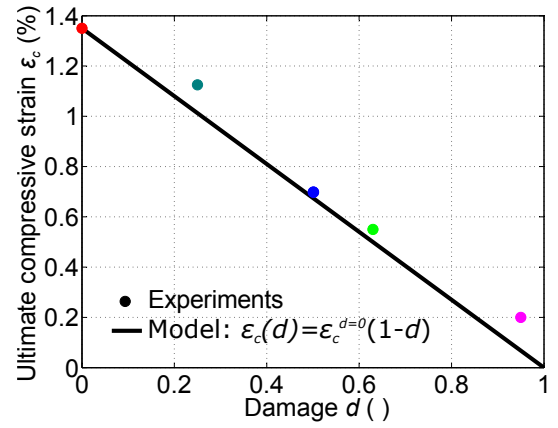

Figure 10: Effect of damage on ultimate compressive strain (woven carbon/epoxy material G939/M18)

($\varepsilon_c^{d=0}$) in the model. This value can be directly measured on an undamaged specimen.

4. Conclusion

In this work, the effect of matrix damage on the compressive strength in fiber direction of laminated composites was investigated experimentally. The specimens used were dumbbell-shaped tubes where fibers were positioned both in the circumferential and axial directions. This type of specimens, usually used for traction or compression tests, also makes it possible to easily introduce damage in the matrix with a cyclic torsional load.

First, the behavior up to failure of undamaged samples was studied. The behavior identified was significantly non linear and comparable to literature results. The ultimate compressive strain seemed to be close to the ultimate tensile strain. Yet the ultimate stress value was significantly lower, in absolute value, because of the non linear behavior of the material.

Second, experiments on fatigue damaged specimens were considered. It appeared that the stiffness in fiber direction is not modified when damage increases. This is due to the fact that the fibers are not broken during the torsional cycles and the compression load path. The most important result concerns the effect of matrix damage on compressive strength. It was indeed shown that damage significantly decreases the ultimate compressive strain. A linear decrease in the ultimate compressive strain was measured. The model proposed was in good agreement with the experimental data and had the great advantage of being directly identified in a compression test on a undamaged specimen.

5. Acknowledgments

6. References

[1] P. Ladeveze, E. Ledantec, Damage modelling of the elementary ply for laminated composites, Composites Science and Technology 43 (3) (1992) 257–267, ISSN 02663538, doi:10.1016/0266-3538(92)90097-M.

[2] J. Payan, C. Hochard, Damage modelling of laminated carbon/epoxy composites under static and fatigue loadings, International Journal of Fatigue 24 (2) (2002) 299–306.

[3] C. Hochard, Y. Thollon, A generalized damage model for woven ply laminates under static and fatigue loading conditions, International Journal of Fatigue 32 (1) (2010) 158–165.

[4] C. Hochard, S. Miot, Y. Thollon, N. Lahellec, J.-P. Charles, Fatigue of laminated composite structures with stress concentrations, Composites Part B: Engineering 65 (0) (2014) 11 – 16, ISSN 1359-8368, doi: http://dx.doi.org/10.1016/j.compositesb.2013.10.020.

[5] Y. Thollon, Analyse du comportement à rupture de composites stratifiés constitués de plis tissés sous chargements statique et de fatigue, Ph.D. thesis, Aix-Marseille Université - Laboratoire de Mécanique et d'Acoustique, France, 2009.

[6] A. Gibson, M. O. Torres, T. Browne, S. Feih, A. Mouritz, High temperature and fire behaviour of continuous glass fibre/polypropylene laminates, Composites Part A: Applied Science and Manufacturing 41 (9) (2010) 1219–1231, ISSN 1359835X, doi: 10.1016/j.compositesa.2010.05.004.

[7] B. W. Rosen, Mechanics of Composite Strengthening, in: Seminar of the American Society for metals, Ohio, 37–75, 1965.

[8] N. Feld, O. Allix, E. Baranger, J.-M. Guimard, Micro-mechanical prediction of UD laminates behavior under combined compression up to failure: influence of matrix degradation, Journal of Composite Materials 45 (22) (2011) 2317–2333.

[9] B. Budiansky, N. A. Fleck, Compressive failure of fibre composites, Journal of the Mechanics and Physics of Solids 41 (1) (1993) 183–211.

[10] A. S. Argon, Fracture of composites, Treatise on Material Science and Technology 1 (1972) 79–114.

[11] J.-C. Grandidier, P. Casari, C. Jochum, A fibre direction compressive failure criterion for long fibre laminates at ply scale, including stacking sequence and laminate thickness effects, Composite Structures 94 (12) (2012) 3799–3806, ISSN 02638223, doi: 10.1016/j.compstruct.2012.06.013.

[12] S. Kulkarni, J. Rice, B. Rosen, An investigation of the compressive strength of Kevlar 49/epoxy composites, Composites 6 (5) (1975) 217–225.

[13] P. S. Steif, A simple model for the compressive failure of weakly bonded, fiber-reinforced composites, Journal of composite materials 22 (9) (1988) 818–828.

[14] D. Adams, Current compression test methods, High-Performance Composites 3 (2005) 40–41.

[15] O. Montagnier, C. Hochard, Compression Characterization of High-modulus Carbon Fibers, Journal of Composite Materials 39 (2005) 35–49.

[16] M. M. Shokrieh, M. J. Omidi, Compressive response of glass-fiber reinforced polymeric composites to increasing compressive strain rates, Composite Structures 89 (4) (2009) 517–523, ISSN 02638223, doi: 10.1016/j.compstruct.2008.11.006.

[17] J. Lee, C. Soutis, A study on the compressive strength of thick carbon fibre-epoxy laminates, Composites science and technology 67 (10) (2007) 2015–2026.

[18] N. A. Fleck, Compressive failure of fiber composites, Advances in applied mechanics 33 (1997) 43–117.

[19] O. Allix, P. Ladevèze, E. Vittecoq, Modelling and identification of the mechanical behaviour of composite laminates in compression, Composites science and technology 51 (1) (1994) 35–42.

[20] N. De Carvalho, S. Pinho, P. Robinson, An experimental study of failure initiation and propagation in 2D woven composites under compression, Composites Science and Technology 71 (10) (2011) 1316–1325, ISSN 02663538, doi:10.1016/j.compscitech.2011.04.019.

[21] S. Pinho, P. Robinson, L. Iannucci, Developing a four point bend specimen to measure the mode I intralaminar fracture toughness of unidirectional laminated composites, Composites Science and Technology 69 (7-8) (2009) 1303–1309, ISSN 02663538, doi: 10.1016/j.compscitech.2009.03.007.

[22] C. Bois, O. Montagnier, C. Hochard, Caractérisation du comportement en compression des matériaux composites par essais de flexion pure, in: 15eme Journées Nationales des composites, 107–114, 2007.

[23] M. R. Wisnom, J. W. Atkinson, Constrained buckling tests show increasing compressive strain to failure with increasing strain gradient, Composites Part A: Applied Science and Manufacturing 28 (11) (1997) 959–964.

[24] S. Drapier, C. Gardin, J. C. Grandidier, M. Potier-Ferry, Structure effect and microbuckling, Composites science and technology 56 (7) (1996) 861–867.

[25] G. Eyer, Rupture des matériaux composites en compression sens fibre. Analyse de l'effet de l'endommagement., Ph.D. thesis, Université d'Aix-Marseille, 2015.

[26] G. Eyer, C. Hochard, O. Montagnier, J.-P. Charles, Effect of transverse damage on compressive strength in fiber direction for CFRP, in: European Conference on Composites Materials, Sevilla, 2014.

[27] G. Eyer, O. Montagnier, J.-P. Charles, C. Hochard, Design of a composite tube to analyze the compressive behavior of CFRP, Composites Part A: Applied Science and Manufacturing In press, doi:10.1016/j.compositesa.2016.04.006.

[28] J. Raasch, Table rolling produces durable, large diameter aircraft ducts, High-Performance Composites 3 (1998) 35–37.

[29] Aramis, Aramis v5. 4 user manual, URL http://www.gom.com, 2005.

[30] The MathWorks, MATLAB, The MathWorks Inc., http://www.mathworks.com, 1990.

[31] C. Hochard, J. Payan, O. Montagnier, Design and computation of laminated composite structures, Composites science and technology 65 (3) (2005) 467–474.

[32] G. Eyer, O. Montagnier, C. Hochard, J.-P. Charles, F. Mazerolle, Influence de l'alignement des fibres sur la rupture des composites en compression sens fibre, in: Journées Nationales des composites, Villeurbanne, 2015.